Journal of Thermal Analysis, Vol. 49 (1997) 407-415

COMPATIBILITY OF TIRE ELASTOMERS USING DERIVATIVE HEAT FLOW TRACES IN THE GLASS TRANSITION REGION

A. K. Sircar, M. L. Galaska and R. P. Chartoff

Center for Basic and Applied Polymer Research, University of Dayton, Dayton, OH 45469, USA

Abstract

Derivative heat flow curves give much more information about the phase heterogeneity of binary blends composed of NR, SBR and BR elastomers than T_g. In blend compositions, the areas under the derivative heat flow curves appear to be an additive function of the concentration of elastomers in the case of incompatible blends (NR/BR, NR/SBR). They are less than additive for either a partially compatible blend (uncured SBR/BR) or a compatible blend (covulcanized SBR/BR). In the case of 60/40 SBR/BR blends, a DSC ($T_{0.5}$) reveals a single T_g, in conformity with the earlier investigators, whereas the derivative heat flow curve shows two peaks (T_p) indicating incomplete homogenization of the phases. This is a new observation not mentioned in the published literature. Thus, derivative heat flow traces are likely to provide a unique tool to determine compatibility of elastomers. The study also reveals the importance of sample contact with the DSC pan in quantitative determinations.

Keywords: compatibility, covulcanization, derivative heat flow ($\Delta W/\Delta T$), DSC, microheterogeneous

Introduction

A previous publication [1] describes the advantage of using derivative heat flow peak (T_p), as compared to either the extrapolated onset (T_{eo}) or midpoint of glass transition temperature ($T_{0.5}$) curve of elastomers. This study indicates that it should be possible to determine compatibility of elastomer blends from the additivity of peak areas in the glass transition temperature region. The present study extends the previous work to some technically important elastomers and blends that are widely used in the tire tread and sidewall compositions with a view to confirm the usefulness of the derivative heat flow ($\Delta W/\Delta T$, cal s^{-1} g^{-1}) method to determine compatibility of elastomers.

Experimental

Materials

The elastomers BR [*cis*-poly(butadiene) rubber, (Budene 1207)], SBR 1500 (low-temperature emulsion copolymer of styrene/butadiene, 25/75 nominal ratio),

0368–4466/97/ $ 5.00

John Wiley & Sons Limited
Chichester

and NR [natural rubber (SMR-5, a grade of Standard Malaysian Rubber)] used are commercial samples and were used as received. Carbon black, curatives, oil and other ingredients used for compounding of rubber are all industrial samples and were used as received. The recipes used are all ASTM recommendations (ASTM D3181, 3185, 3189, 3192, 3568) with minor modifications, if necessary. The mixed compounds were cured into 3 mm slabs at times and temperatures indicated in Table 1.

T_g measurements

A TA Instruments 2910 DSC, under nitrogen purge and a heating rate of 10°C min^{-1}, was used for T_g measurements. Low temperature calibration of the instrument at the same rate of heating was carried out with cyclohexane at −82°C (transitions, 6.55 and −82°C). Samples of suitable diameter were bored out using a cork borer and pressed to as thin a film as possible in order to have a large surface area. All samples (cured or uncured) were annealed at 100°C for 15 min under nitrogen purge and quenched (30°C min^{-1}) by pouring liquid nitrogen into the DSC cover to −140°C. Annealing at 100°C for 15 min should not initiate curing of the uncured stocks or cause further curing of the vulcanizates. T_g was determined at half-height as well as at the peak of the ($\Delta W/\Delta T$) curve, where $\Delta W/\Delta T$ represents the variation of heat capacity in watts per degree change in temperature. Reproducibility of the peak temperature is very good. For example, the standard deviations for five determinations of T_g for four different samples of NBR-50 at 10°C min^{-1} were ±0.41, 0.56, 0.68 and 0.41°C. However, reproducibility of the areas under the ($\Delta W/\Delta T$) peak is not as good. The individual data deviates from the linear fit average value for NR, SBR and BR by ±3.5%, ±7.3%, and ±8.4%, respectively. Because of the large error, all peak area data were repeated at least three times and averaged.

Results and discussion

Most passenger tire treads in the U.S. are made of either BR, SBR, or SBR/BR blend, with BR varying from 25% to 50% of the total polymer in the blend. Truck tire treads are mostly binary and tertiary blends containing varying proportions of NR, added to improve hysteresis properties. A comprehensive survey of the tire side walls [2] from various manufactures in U.S. shows that they contain the following elastomers: SBR, SBR/BR, NR/BR, NR/SBR and NR/SBR/BR. The present study includes these technically important blends except for the tertiary NR/SBR/BR blend.

Figure 1 illustrates an NR T_g trace where T_g is determined both at half-height ($T_{0.5}$) and at the peak of the ($\Delta W/\Delta T$) curve. An unusual feature of the NR T_g curve is the small dip at the high-temperature end, characteristic of an enthalpy relaxation [3]. Enthalpy relaxation is generally observed when the cooling rate is slower than the heating rate. However, slow heating of the quenched sample within the practical range of this study (up to 5°C min^{-1}) failed to eliminate this feature. The dip is much less for blends and vulcanized samples and caused no insurmountable problem for this study.

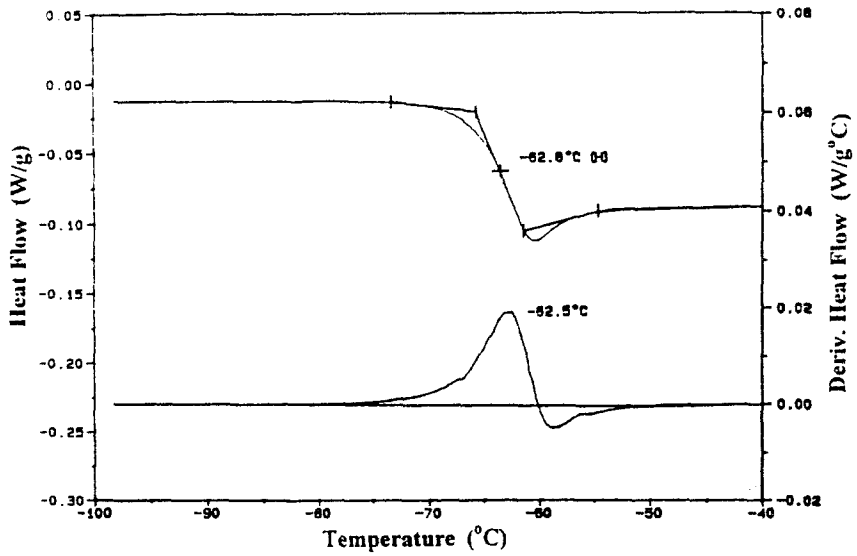

Fig. 1 Glass transition of natural rubber showing $T_{0.5}$ and T_p

A linear relationship was observed in this study for weight of BR, SBR or NR undergoing T_g transition and the corresponding ($\Delta W/\Delta T$) areas. It was also observed that ΔC_p follows a linear relationship with the derivative heat flow data. Thus, ($\Delta W/\Delta T$) areas may be used for quantitative determinations of the amorphous portion of the elastomer, much like the use of ΔC_p for this purpose [4]. This is also similar to the use of DTG peak area for quantitative estimation of mass loss in TG.

The derivative heat flow curve area increases with increasing heating rate. The extrapolated plot of heating rate *vs.* ($\Delta W/\Delta T$) area passes through zero, indicating that the area would be zero at zero heating rate. Therefore, a high heating rate would be beneficial for this study. However, high heating rate also increases machine noise. Therefore, a heating rate of 10°C min^{-1} was chosen as a compromise.

Single elastomers

Table 1 presents the data from T_g experiments. All elastomers were tested raw, compounded uncured and compounded cured states. As shown in Table 1, T_g increases as the elastomers are immobilized by the fillers even in the uncured state (samples 2, 5 and 8) and a further increase of T_g was observed as the chain mobility is further reduced by vulcanization (samples 3, 6 and 9). T_g's, determined at half-height and at the ($\Delta W/\Delta T$) peak, are practically identical. The merits and demerits of using the ($\Delta W/\Delta T$) peak for determining T_g have been discussed before [1].

A remarkable observation is that the ($\Delta W/\Delta T$) peak area per gram of the elastomer is increased about two and a half time for the uncured carbon black loaded BR and SBR samples as compared to the raw sample. The increase is about two times for NR. This is both an advantage and a disadvantage. A larger area increases the sensitivity and accuracy of the experiments, but the different areas for the same

Table 1 T_g[a] of elastomers and blends using DSC ($T_{0.5}$) and derivative heat flow curve maximum (T_p)

Sample #/ Elastomer	State of loading or cure	$T_{0.5}$/ °C	T_p/ °C	($\Delta W/\Delta T$) Area×10^3/cal (s g)$^{-1}$	Calc. Additive value for ($\Delta W/\Delta T$) Area×10^3/cal (s g)$^{-1}$
1. BR	unloaded uncured	–104.1	–104.3	13.60	13.60
2. BR	50 phr N330 carbon black, uncured	–98.1	–98.8	34.93	34.93
3. BR	60 phr N330 carbon black, cured 35 min @ 293°F	–96.3	–96.7	35.76	35.76
4. SBR	unloaded uncured	–50.5	–50.6	18.76	18.76
5. SBR	50 phr N330 carbon black, uncured	–48.8	–50.2	46.57	46.57
6. SBR	50 phr N330 carbon black, cured 70 min @ 293°F	–42.7	–43.6	48.20	48.20
7. NR	unloaded uncured	–62.8	–62.5	19.11	19.11
8. NR	50 phr N330 carbon black, uncured	–59.5	–59.1	36.70	36.70
9. NR	50 phr N330 carbon black, cured 30 min @ 293°F	–55.6	–55.6	35.94	35.94
10. BR/NR (50/50)	unloaded uncured	–106.8 –64.7	–104.0 –63.9	29.96 31.60	13.60 19.11
11. NR/SBR (50/50)	unloaded uncured	–61.3 –51.4	–61.9 –50.9	30.90 24.90	19.11 18.76
12. SBR/BR (50/50)	unloaded uncured	–104.3 –53.6	–103.0 –52.9	13.10 19.90	13.60 18.76
13. SBR/BR (60/40)	50 phr N330 carbon black, uncured	–103.2	–102.9	5.48	25.51[b]
14. SBR/BR (60/40)	50 phr N330 carbon black, cured 40 min @ 320°F	–85.12	–92.4 –82.3	5.00	26.30[b]

[a] T_g determined at half-height. Samples annealed at 100°C for 5 min then cooled at maximum rate with gas from liquid nitrogen reservoir.

[b] Calculated total area from component polymer weight.

elastomer in raw and compounded state require that experimental curves be compared with reference curves in the same state of the elastomer. The most probable explanation of this phenomenon is as follows: Most elastomers in the raw state are porous and nervy. It is pretty difficult to make a film with a large surface area that will lay flat in the DSC pan with this nervy sample. The reverse is true for both the

uncured and cured compounds. Thus, the larger ($\Delta W/\Delta T$) area may be ascribed to more intimate contact as well as large surface area of these samples, which could be pressed to a thin film. The importance of thermal contact with the pan to obtain quantitative data was also demonstrated by Goh [5] who used solvent-cast samples and obtained much higher enthalpy values for degradation of NR and gutta-percha in oxygen than those reported earlier [6].

Incompatible elastomer blends

Incompatible blends studied are NR/BR and NR/SBR. In these cases, the domain sizes are sufficiently big and the restriction of movement by cross-links has little effect on the motion of polymer chains within the larger domains. Figure 2 shows two distinct glass transitions for NR/BR (sample 10) and NR/SBR (sample 11) in the raw state. This is an indication of their incompatibility. The incompatibility for NR/SBR persists for the loaded as well as the cured compound (not shown in Table 1). Their ($\Delta W/\Delta T$) areas in Table 1 (column 5) show that the experimental areas are bigger than the areas for the single elastomers. As mentioned before, similar observations are also true for NR/NBR-50 and NBR-50/NBR-21 blends studied earlier [1]. Thus, the present data lend further support to the proposition that for incompatible elastomer blends the sum of the ($\Delta W/\Delta T$) areas is equal or greater than that of the individual component elastomers.

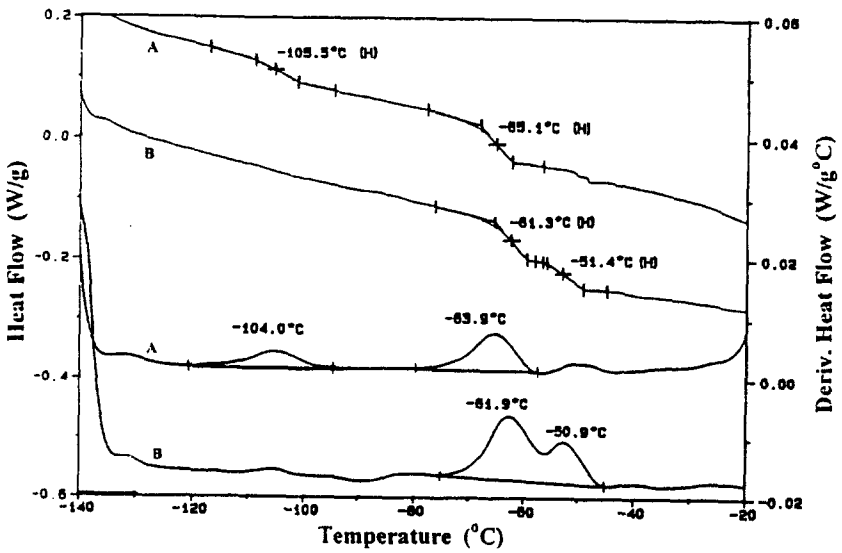

Fig. 2 DSC T_g and the corresponding ($\Delta W/\Delta T$) curve for 50/50 uncured and loaded blends: A. NR/BR and B: NR/SBR

Compatible elastomer blends

It is well known that, whithout specific interactions, polymers are rarely thermodynamically compatible. Literature surveys reveal only a few examples of com-

patible rubber blends [7, 8]. The SBR/BR blend is often referred in the literature [2, 9–13] as a compatible system, especially in the cured state. The SBR/BR blend system is popular in the elastomer industry because it combines the good hysteresis properties of BR with the abrasion resistance of SBR in the tire tread. Earlier DTA or DSC studies for this system were limited by the fact that very diffuse T_g interval was obtained for cured BR/SBR that is difficult to detect.

T_g trace for BR suffers from the complication that they show exothermic cold crystallization as well as crystalline melting peaks [10, 14]. This is shown in Fig. 3. The above phenomena have adverse consequences for determining T_g of this elastomer and its blends. Because of the partial crystallinity, the amorphous part of this elastomer is reduced resulting in a weak T_g trace. Also, the cold crystallization occurs around –60 to –45°C range. This is where SBR T_g should show up, but it is completely masked by BR cold crystallization peak. The extent of cold crystallization and crystallinity are susceptible to the annealing procedure which alters the amount of amorphous portion of the elastomer and consequently ΔC_p and $(\Delta W/\Delta T)$ area. Thus, rigid adherence to the annealing procedure must be maintained in order to obtain reproducible data. Also, carbon black and SBR, if present, reduces crystallinity by immobilization of the BR chains. Crystallization is almost completely eliminated on vulcanization.

Table 1 (column 5) shows that raw SBR/BR (50/50) (sample 12) exhibits two T_g's for BR and SBR. The temperature of the T_g's is more or less unaltered. This indicates two phases. Also, the areas under BR and SBR $(\Delta W/\Delta T)$ peaks match those for the reference samples as expected for an incompatible blend. This indicates again that $(\Delta W/\Delta T)$ area can be used as a measure of compatibility.

Fifty phr N330 loaded uncured SBR/BR (60/40) (sample 13) compound shows only the BR T_g at a slightly higher temperature. $(\Delta W/\Delta T)$ area indicates at least par-

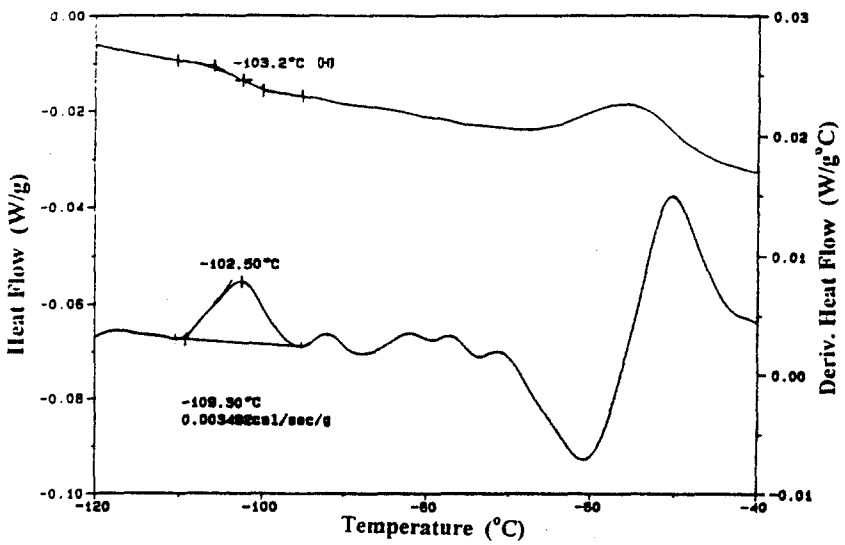

Fig. 3 DSC T_g and corresponding $(\Delta W/\Delta T)$ curve for uncured 60/40 SBR/BR blend containing 50 phr N330 carbon black in ASTM D3187 recipe

tial compatibility, but cannot be confirmed because of the interference shown in Fig. 3. However, the fact that the BR T_g remains unchanged suggests that the elastomers in sample 13 are incompatible. It is surprising the SBR/BR raw blend does not show the interference due to BR crystallinity.

The cured SBR/BR (Fig. 4, sample 14) shows a T_g at −85°C, intermediate between the T_g's of the two components, in agreement with the earlier data of Sircar and Lamond [2] and Burfield and Lim [3]. The T_g value is very close to that calculated from the Fox equation [15] (−82.5°C *vs.* −85°C). Interestingly, the $(\Delta W/\Delta T)$ curve shows two peaks at −92°C and −82°C. This indicates residual heterogeneity between the phases. The total area under the $(\Delta W/\Delta T)$ peaks is much smaller than the calculated value (Table 1, column 6) indicating compatibility.

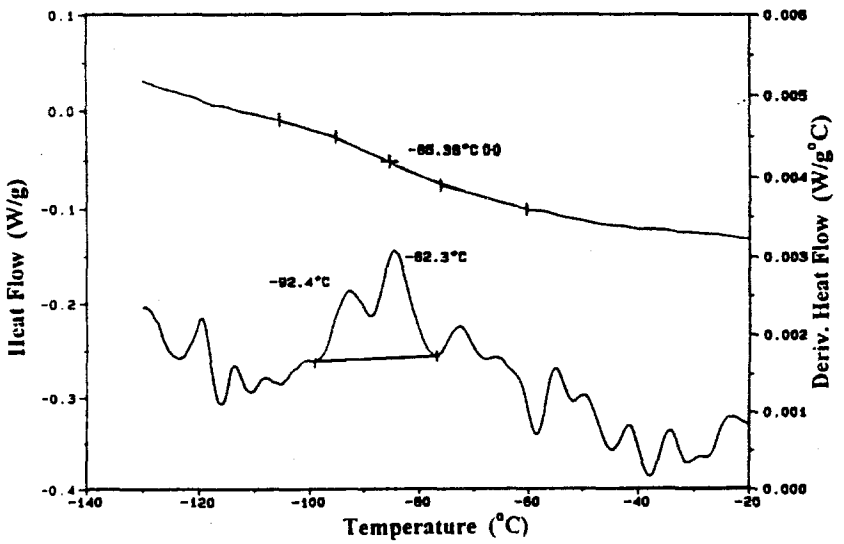

Fig. 4 DSC T_g and the corresponding $(\Delta W/\Delta T)$ curve for cured 60/40 SBR/BR blend containing 50 phr N330 carbon black in ASTM D3187 recipe

On the basis of special electron microscope technique whereby the contrast was greatly enhanced and discrete zones were observed for gum blends of 50:50 SBR/BR, Callan *et al.* [13], suggest that uncured BR-SBR blends are microheterogeneous with very small domain sizes. These small domain sizes are capable of covulcanization and thus give a single T_g when cured. This leads to a broadening of the thermal response, giving a diffuse T_g interval that is difficult to detect by DSC. In more heterogeneous systems, the separate domains are sufficiently large that the response is less sensitive to the restriction imposed by cross-linking.

When the domain size of the component elastomer is sufficiently small (Kaplan [15] suggests 150 Å), the thermal or mechanical response becomes insensitive to heterogeneity. For example, when the domain size of NR-*cis*-polypentenamer is 50–100 Å, the torsion pendulum shows only single intermediate T_g [16]. Roland [17] observed a very broad T_g for NR and 1,4-BR blend covering several decades

of frequency region. He suggests that NR/BR blend develops a broad interconnected interface region upon vulcanization. This can cause disappearance of the expected distinct glass transition. There are many examples of covulcanization and consequent appearance of a single T_g on the literature [18–21]. It appears from the example in 60/40 SBR/BR system in this study that ($\Delta W/\Delta T$) traces can detect the two phases even in microheterogeneous binary blends where some other techniques (DSC, DMA) may fail.

Conclusions

The study shows the advantages of simultaneous recording DSC T_g and ($\Delta W/\Delta T$) curves to determine glass transition temperature and to detect discrete phases not observed by DSC curves. Several prominent observations are as follows:

1) Importance of sample contacting the DSC pan in T_g experiments is revealed by the much larger ($\Delta W/\Delta T$) area for loaded as well as vulcanized samples as compared to raw elastomers.

2) ($\Delta W/\Delta T$) curves for the binary incompatible blends have areas which are additive or more than additive functions of the concentration of the individual components. The ($\Delta W/\Delta T$) curves for the compatible binary blends have areas that are much less than the additive value.

3) Glass transition temperature determined at half-height of DSC T_g traces is almost identical to that determined from the peak temperature of ($\Delta W/\Delta T$) curves.

4) The implications of having a partially crystalline component such as BR in the BR/SBR blend system have been explained.

5) ($\Delta W/\Delta T$) curves can reveal separate T_g's for binary systems having close T_g regions where DSC alone cannot.

6) Finally, covulcanization of 60/40 SBR/BR blend reveals a single phase by DSC but two separate phases by ($\Delta W/\Delta T$) traces. Thus, ($\Delta W/\Delta T$) traces are able to detect distinct phases in co-vulcanized microheterogeneous blends where other techniques may fail.

7) ($\Delta W/\Delta T$) curves can be useful in studies correlating phase heterogeneity and physical property in microheterogeneous blends for elastomers used in tires.

8) Reproducibility of the peak areas is poor. This seems to be the limitation of the method.

References

1 A. K. Sircar, M. L. Galaska, S. M. Linden, B. Kumar, R. P. Chartoff and L. G. Scanlon, Proc. 22nd North Amer. Therm. Anal. Soc., Denver, 1993, p. 319–324.
2 A. K. Sircar and T. G. Lamond, Rubber Chem. Technol., 48 (1975) 301.
3 D. R. Burfield and K. L. Lim, Macromolecules, 16 (1983) 1170.
4 H. Bair, in 'Thermal Characterization of Polymeric Materials,' E. A. Turi, Ed.: Academic Press, New York 1982.
5 S. H. Goh, Thermochim. Acta, 39 (1980) 353.
6 M. A. Ponce-Vélez and E. Campos-López, J. Appl. Polym. Sci., 22 (1978) 2485.
7 S. Krause, J. Macromol. Sci. Re. Macromol. Chem., C7, 251.

8 W. M. Hess, C. R. Herd and P. C. Vegvari, Rubber Chem. Technol., 66 (1993) 329.
9 M. H. Walters and D. N. Keyte, Trans. Inst. Rubber Ind., 38 (1962) 40.
10 P. A. Marsh, A. Voet and L. D. Price, Rubber Chem. Technol., 40 (1967) 359.
11 P. A. Marsh, A. Voet, L. D. Price and T. J. Mullen, Rubber Chem. Technol., 41 (1967) 344.
12 J. B. Gardiner, Rubber Chem. Technol., (1970), 43–370.
13 J.E. Callan, W. M. Hess and C. E. Scott, Rubber Chem. Technol., 44 (1971) 814.
14 A. K. Sircar and T. G. Lamond, Rubber Chem. Technol., 46 (1973) 178.
15 T. G. Fox, Bull. Am. Phys. Soc., 1 (1956) 123.
16 D. S. Kaplan, J. Appl. Polym. Sci., 20 (1976) 2615.
17 H. G. Braun and G. Rehage, Angew. Makromol. Chem., 131 (1985) 107.
18 N. K. Dutta and D. K. Tripathy, J. Elastomers Plast., 25 (1993) 158.
19 H. J. Radusch, E. Lämmer, E. Spirk and M. Dudik, Kautsch. Gummi. Kuntstst., 46 (1993) 703.
20 R. F. Bauer and E. A. Dudley, Rubber Chem. Technol., 50 (1977) 35.
21 T. Inoue, F. Shomura, T. Ougizawa and K. Miyasaka, Rubber Chem. Technol., 58 (1985) 873.